THE JOURNAL OF BIOLOGICAL CHEMISTRY VOL. 281, NO. 48, pp. 36819–36827, December 1, 2006

Surface Charge Interactions of the FMN Module Govern Catalysis by Nitric-oxide Synthase*[S]

Received for publication, June 27, 2006, and in revised form, September 18, 2006 Published, JBC Papers in Press, September 25, 2006, DOI 10.1074/jbc.M606129200

Koustubh Panda[‡1], Mohammad Mahfuzul Haque[‡1], Elsa D. Garcin-Hosfield[§], Deborah Durra[‡], Elizabeth D. Getzoff[§], and Dennis J. Stuehr[‡2]

From the [‡]Department of Pathobiology, Lerner Research Institute, Cleveland Clinic, Cleveland, Ohio 44195 and the [§]Department of Molecular Biology, Skaggs Institute for Chemical Biology, The Scripps Research Institute, La Jolla, California 92037

The FMN module of nitric-oxide synthase (NOS) plays a pivotal role by transferring NADPH-derived electrons to the enzyme heme for use in oxygen activation. The process may involve a swinging mechanism in which the same face of the FMN module accepts and provides electrons during catalysis. Crystal structure shows that this face of the FMN module is electronegative, whereas the complementary interacting surface is electropositive, implying that charge interactions enable function. We used site-directed mutagenesis to investigate the roles of six electronegative surface residues of the FMN module in electron transfer and catalysis in neuronal NOS. Results are interpreted in light of crystal structures of NOS and related flavoproteins. Neutralizing or reversing the negative charge of each residue altered the NO synthesis, NADPH oxidase, and cytochrome *c* reductase activities of neuronal NOS and also altered heme reduction. The largest effects occurred at the NOS-specific charged residue Glu[762]. Together, the results suggest that electrostatic interactions of the FMN module help to regulate electron transfer and to minimize flavin autoxidation and the generation of reactive oxygen species during NOS catalysis.

Nitric oxide is an important biological signal molecule produced in animals by three nitric-oxide synthase (NOS)[3] isozymes: inducible NOS (iNOS), neuronal NOS (nNOS), and endothelial NOS (eNOS) (1, 2). NOS enzymes have unique characteristics, and their protein structure-function relationships are of current interest. All mammalian NOS enzymes are comprised of an N-terminal oxygenase domain and a C-terminal flavoprotein domain, with a calmodulin (CaM)-binding site connecting the two domains (3). During NO synthesis, the flavoprotein domain transfers NADPH-derived electrons through its FAD and FMN cofactors to a heme located in the oxygenase domain. This enables NOS to catalyze heme-dependent oxygen activation and a stepwise conversion of L-Arg to NO and citrulline (4, 5). CaM binding to NOS activates NO synthesis by triggering electron transfer from the FMN to the heme (6). CaM also relieves repression of NOS flavoprotein electron transfer to external acceptors like cytochrome *c* (7–9). How these processes occur is mostly unknown.

The nNOS flavoprotein domain (nNOSr) is similar to dual-flavin oxidoreductases like cytochrome P450 reductase (10), novel reductase-1 (11), and methionine synthase reductase (12) and to the flavoprotein domain of bacterial cytochrome P450BM3 (13, 14). All are comprised of a ferredoxin-$NADP^+$ reductase (FNR) module that contains FAD and that binds NADPH, a connecting subdomain that is inserted into the FNR module, and an FMN module. All transfer NADPH-derived electrons to native hemeprotein acceptors (NOS and cytochrome P450BM3) or to artificial hemeprotein acceptors like cytochrome *c*. In nNOS, the electron transfer process appears to involve a conformational equilibrium of the FMN module (9, 15, 16), which is illustrated in Fig. 1. The FMN module must dock with the FNR module in an "FMN-shielded" conformation to receive electrons from FAD. Thereafter, the FMN module must swing away by means of a flexible linker to populate an "FMN-deshielded" conformation to interact with electron acceptors like the NOS oxygenase domain and cytochrome *c*. The crystal structure of nNOSr (15) depicts the FMN module docked against the FNR module in the electron-accepting, FMN-shielded conformation (Fig. 2). A similar arrangement is observed in the crystal structure of cytochrome P450 reductase (10), suggesting that a conformational switching mechanism is likely to operate in related flavoproteins.

The conformational switching model implies that electron transfer into and out of the FMN module is mutually exclusive and probably subject to complex control. How any flavoprotein controls this process is largely unclear (17). For nNOS, the equilibrium between the FMN-shielded and FMN-deshielded conformations appears to have an intrinsic set point that can be influenced by several factors. For example, CaM binding shifts the equilibrium toward the FMN-deshielded conformation (16, 18), whereas the FMN-shielded conformation is stabilized by residues in or near a C-terminal tail regulatory element in conjunction with bound NADPH (15, 16, 18, 19). Shifting the conformational equilibrium of the FMN module in nNOS directly impacts its cytochrome *c* reductase activity and, in some cases, alters the susceptibility of its reduced flavins to autoxidation (16, 19).

* This work was supported by National Institutes of Health Grants GM51491, CA53914, and HL76491 (to D. J. S.) and Grant HL58883 (to E. D. G.). The costs of publication of this article were defrayed in part by the payment of page charges. This article must therefore be hereby marked "*advertisement*" in accordance with 18 U.S.C. Section 1734 solely to indicate this fact.

[S] The on-line version of this article (available at http://www.jbc.org) contains supplemental Tables S1 and S2.

[1] Both authors contributed equally to this work.

[2] To whom correspondence should be addressed: Dept. of Pathobiology, Lerner Research Inst./NC22, Cleveland Clinic, 9500 Euclid Ave., Cleveland, OH 44195. Tel.: 216-445-6950; Fax: 216-636-0104; E-mail: stuehrd@ccf.org.

[3] The abbreviations used are: NOS, nitric-oxide synthase; nNOS, neuronal nitric-oxide synthase; CaM, calmodulin; nNOSr, neuronal nitric-oxide synthase flavoprotein domain; FNR, ferredoxin-$NADP^+$ reductase; EPPS, 4-(2-hydroxyethyl)-1-piperazinepropanesulfonic acid; L-Arg, L-Arginine.

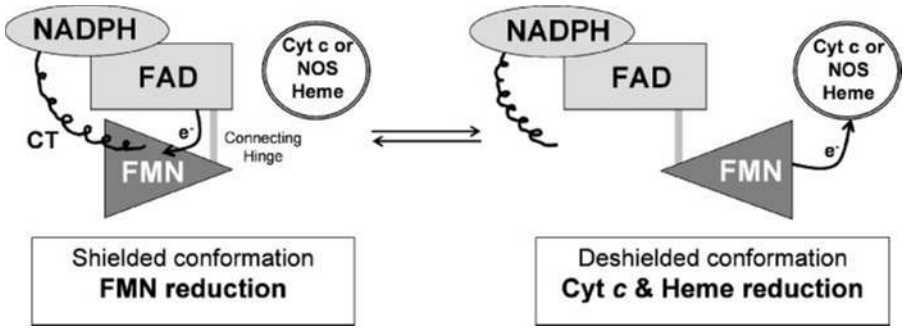

FIGURE 1. **Conformational equilibrium of the nNOSr FMN module.** The diagram illustrates a conformational equilibrium that may control the electron transfer reactions of the FMN module (*triangle*). The module is expected to swing back and forth to contact the FNR module (*upper left*) and an electron acceptor like cytochrome *c* (*Cyt c*) or NOS heme (*circle*). The C-terminal tail (*CT*) is thought to affect the equilibrium by physically stabilizing the FMN-shielded conformation. This figure has been adapted from Ref. 19.

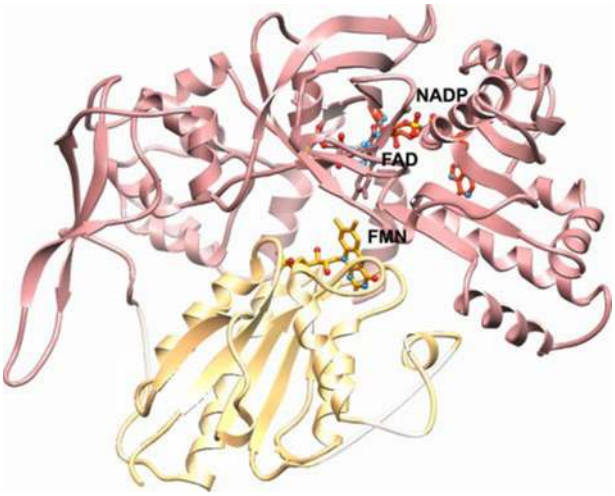

FIGURE 2. **Structure of nNOSr.** The ribbon diagram shows the FMN module (*yellow*) docked against the FNR module (*pink*) in the FMN-shielded conformation, with bound cofactors FMN, FAD, and NADP shown in ball-and-stick representation.

Variables that may control FMN module function in nNOS and related flavoproteins include surface hydrophobic and electrostatic contacts, hinge length and flexibility, and thermodynamic stability of reduced flavin states (15, 20–25). Charged residues at the FMN module interface are prominent in the crystal structure of nNOSr (15) and may be important for function as judged by experiments demonstrating salt effects on nNOS catalysis (26, 27). Six acidic residues create an electronegative patch on the surface of the FMN module in nNOSr (Fig. 3*A*). This electronegative patch interacts with a complementary electropositive patch on the surface of the FNR module (Fig. 3*B*). A closer view of how these residues interact is shown in Fig. 3*C*. Similar electrostatic complementation is present to varying degrees in related flavoproteins, suggesting that it may be a general means to control subdomain interactions. NOS oxygenase domains also contain an electropositive surface patch (Fig. 3*D*) in an area considered to be a potential docking site for the FMN module (28). Thus, electrostatic interactions could conceivably regulate both the electron import and export reactions of the FMN module during NOS catalysis. We therefore employed point mutagenesis to neutralize or reverse the charges of the six acidic residues that create the electronegative patch on the FMN module, along with the interactions of one residue in the complementary electropositive surface patch of the FNR module, as listed in Table 1. The results obtained with these mutants support a role for electrostatic surface interactions in controlling electron transfer, O_2 reduction, and catalysis in nNOS and reveal which residues are the most important.

EXPERIMENTAL PROCEDURES

Reagents—All reagents and materials were obtained from Sigma or sources reported previously (29–31).

Molecular Biology—Wild-type and mutant nNOS proteins containing a His_6 tag attached to their N termini were overexpressed in *Escherichia coli* strain BL21(DE3) using a modified pCWori vector as described (32). Restriction digestions, cloning, and bacterial growth was performed using standard procedures. Transformations were done using a TransformAid bacterial transformation kit (Fermentas). Oligonucleotides used to construct site-directed mutants in nNOS were obtained from Integrated DNA Technologies (Coralville, IA) and are listed in supplemental Table S1. Site-directed mutagenesis was done using a QuikChange XL site-directed mutagenesis kit (Stratagene, La Jolla, CA). Incorporated mutations were confirmed by DNA sequencing at the Cleveland Clinic Molecular Biotechnology Core.

Expression and Purification of nNOS Proteins—All proteins were purified in the presence of (6*R*)-tetrahydrobiopterin and L-Arg as described previously (29, 33). The ferrous heme-CO adduct absorbing at 444 nm was used to measure hemeprotein content with an extinction coefficient of $\epsilon_{444} = 74\ mM^{-1}\ cm^{-1}$ (A_{444}–A_{500}).

Measurement of Flavin Content—Bound FAD and FMN were released from nNOS proteins by heat denaturation of the enzyme (95 °C for 5 min in the dark) in sealed and light-protected tubes. The samples were then cooled to 4 °C and filtered to remove denatured protein. Filtrates were injected onto an Alltech Partisil ODS-3 column (250 × 4.6 mm, 5 μm) and subjected to binary gradient elution with 25 mM phosphate buffer (pH 5.8) and 100% acetonitrile at a flow rate of 1 ml/min. FAD and FMN had retention times of 4.1 and 7.6 min, respectively, and the peaks were completely resolved. Flavins were detected by fluorescence emission ($\lambda_{ex} = 460$ nm and $\lambda_{em} = 530$ nm) and quantitated against freshly prepared FAD and FMN standards.

NO Synthesis, NADPH Oxidation, and Cytochrome c Reduction—NO synthesis activity was determined using the spectrophotometric oxyhemoglobin assay (29, 30, 33). Cuvettes contained 0.2 μM nNOS, 40 mM EPPS (pH 7.6), 150 mM NaCl, 0.3 mM dithiothreitol, 4 μM FAD, 4 μM FMN, 10 μM (6*R*)-tetrahydrobiopterin, 10 mM L-Arg, 1 mg/ml bovine serum albumin, 0.8 mM Ca^{2+}, 0.6 mM EDTA, 0.9 μM CaM, 100 units/ml catalase, 25 units/ml superoxide dismutase, and 5 μM oxyhemoglobin. The reaction was initiated with 300 μM NADPH in a total reaction

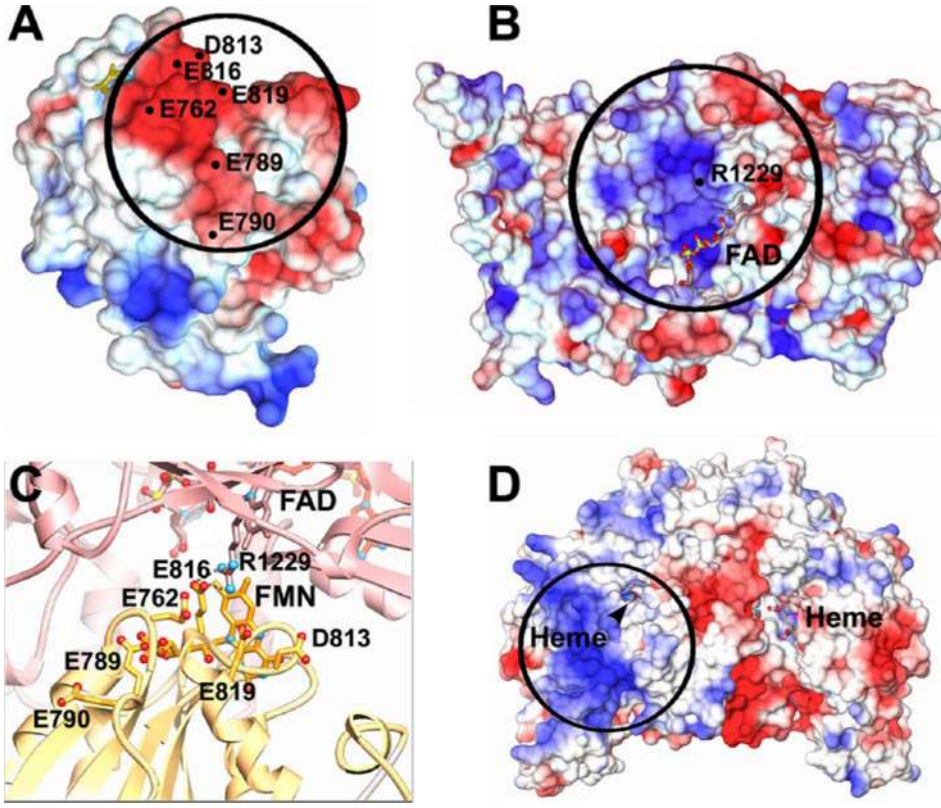

FIGURE 3. **Complementary electrostatic surfaces in nNOS and residue interactions at the FNR/FMN module interface.** *A*, six residues create an electronegative patch on the interacting surface of the FMN module. *B*, the interacting surface of the FNR module contains an electropositive patch, with Arg^{1229} indicated. *C*, shown are details of the FMN module (*yellow*) and FNR module (*pink*) interface, with the indicated residues shown in ball-and-stick representation. *D*, the oxygenase domain of nNOS contains a conserved electropositive surface patch that is located in an area considered to be a potential docking site for the FMN module.

TABLE 1
Mutations used in the study

nNOS mutations
FMN module
Glu^{762} to Asn, Arg, or Ala
Glu^{789} to Asn, Arg, or Ala
Glu^{790} to Asn, Arg, or Ala
Asp^{813} to Asn, Arg, or Ala
Glu^{816} to Asn, Arg, or Ala
Glu^{819} to Asn, Arg, or Ala
FNR module
Arg^{1229} to Asn, Glu, or Ala

volume of 500 μl and was run for 3 min at 25 °C. The NO-mediated conversion of oxyhemoglobin to methemoglobin was monitored at 401 nm and converted to a rate of NO synthesis using a difference extinction coefficient of ϵ_{401} = 38 mM^{-1} cm^{-1}. NADPH oxidation rates were similarly measured at 340 nm in the presence of oxyhemoglobin under identical conditions, and the rate of NADPH oxidation was calculated using an extinction coefficient of ϵ_{340} = 6.2 mM^{-1} cm^{-1}. Cytochrome *c* reductase activity was determined at 550 nm (ϵ_{550} = 21 mM^{-1} cm^{-1}) using an assay mixture containing 40 mM EPPS (pH 7.6), 150 mM NaCl, 4 μM FAD, 4 μM FMN, 0.1 mg/ml bovine serum albumin, 10 μg/ml CaM, 0.6 mM EDTA, 10 units/ml catalase, 25 units/ml superoxide dismutase, and 0.1 mM cytochrome *c*. In the cytochrome *c* reductase assays, the concentration of added NaCl in the buffer was either 0 or 150 mM as indicated. The reaction was initiated by addition of 0.1 mM NADPH.

Heme Reduction—The kinetics of heme reduction were analyzed at 10 °C as described previously (30) using a stopped-flow apparatus and diode array detector (Hi-Tech Ltd. Model SF-61) equipped for anaerobic analysis. Ferric heme reduction was followed by formation of the ferrous heme-CO complex at 444 nm. Reactions were initiated by rapidly mixing an anaerobic, buffered, CO-saturated solution containing either 50 μM NADPH or 5 mM $CaCl_2$ with an anaerobic, buffered, CO-saturated solution containing wild-type or mutant nNOS (5 μM), 100 mM EPPS (pH 7.6), 100 mM NaCl, 10 μM (6*R*)-tetrahydrobiopterin, 5 mM L-Arg, 0.3 mM dithiothreitol, 4 μM CaM, and either 1 mM Ca^{2+} when triggered with NADPH or 50 μM NADPH when triggered with Ca^{2+}. Signal-to-noise ratios were improved by averaging 8–10 individual mixing experiments. The time course of the absorbance change was fit to single or multiple exponential equations using a nonlinear least-square method provided by Hi-Tech Ltd.

RESULTS

Overall Properties of the FMN Module Mutants—In general, the mutations incorporated at the interface of the FNR/FMN modules did not alter protein expression or content of bound FAD, FMN, and heme (data not shown). The only mutant with aberrant properties was R1229E nNOS, which bound poorly to the 2′,5′-ADP affinity column during its purification. Because of this, we did not utilize R1229E nNOS in this study. However, the properties of the other mutants indicated they could be used to evaluate roles for the charged surface residues in nNOS function.

Cytochrome c Reductase Activity in the Absence or Presence of Bound CaM—The cytochrome *c* reductase activity of NOS is repressed in the CaM-free state, and the repression is relieved upon CaM binding (34). We compared the steady-state cytochrome *c* reductase activities of each mutant in the absence and presence of bound CaM. All assays contained superoxide dismutase to ensure we detected only superoxide-independent cytochrome *c* reductase activity, *i.e.* that which involves only a direct electron transfer from the FMN hydroquinone ($FMNH_2$) of nNOS to cytochrome *c* (8, 18). Under CaM-free conditions, most of the mutants had higher cytochrome *c* reductase activities relative to wild-type nNOS (Fig. 4, *left panel*). The most prominent increases were in the Glu^{762} and Glu^{816} mutants.

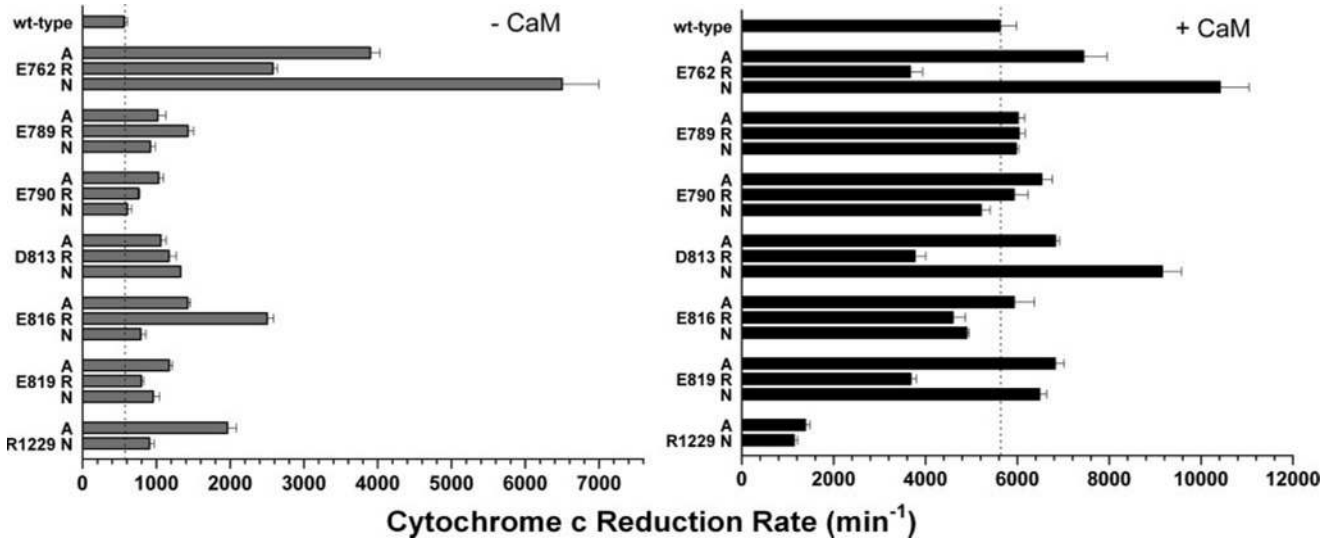

FIGURE 4. **Steady-state cytochrome *c* reductase activities of nNOS and mutants in the absence and presence of CaM.** Activities were measured at 25 °C in the presence of superoxide dismutase and in either the absence (*left panel*) or presence (*right panel*) of CaM. Values are representative of three measurements done under identical conditions using two different protein preparations for each mutant. The *dotted lines* indicate the activity of wild-type (*wt-type*) nNOS.

The relative effect of charge neutralization *versus* charge reversal depended on the acidic surface residue being considered. For example, at Glu^{762}, the rank order of mutational effect was Asn > Ala > Arg, whereas for Glu^{816}, the rank order was Arg > Ala > Asn. Our results show that the electronegative patch residues of the FMN module (particularly Glu^{762} and Glu^{816}) help to repress the cytochrome *c* reductase activity of nNOS in the CaM-free state.

To investigate the importance of charge interaction of each of the six acidic residues, we determined how the two charge-neutralizing mutations (Ala and Asn) at each residue might impact the salt effect on nNOS cytochrome *c* reductase activity. In CaM-free nNOS, a change in salt concentration from 0 to 250 mM is known to double the activity (35), consistent with charge interactions playing a role in repression of the activity. In our hands, the cytochrome *c* reductase activity of CaM-free wild-type nNOS increased by 150 ± 8% ($n = 3$) in going from 0 to 150 mM added NaCl. The charge-neutralizing mutations resulted in a lesser salt effect in at least 7 of 12 cases (supplemental Table S2). A lesser salt effect was observed for both charge-neutralizing mutations at Glu^{762} and Asp^{813} and was observed for at least one of the two charge-neutralizing mutations at Glu^{790}, Glu^{816}, and Glu^{819}, which together represent five of the six charged FMN surface residues that we studied. Charge neutralization did not clearly impact the salt effect in only one case, Glu^{789} (supplemental Table S2). These results suggest that the charge interactions of five of the six acidic surface residues of the FMN module contribute to the overall salt effect on the cytochrome *c* reductase activity of CaM-free nNOS.

The cytochrome *c* reductase activities of the CaM-bound mutants are shown in Fig. 4 (*right panel*). Each FMN domain mutant had an increase in activity relative to the CaM-free condition, indicating that they all still responded to CaM. Most of the mutants achieved activities that were similar (±20%) to those of CaM-bound nNOS. The exceptions were the E762A, E762N, and D813N mutants, whose activities were 130%, 180%, and 160%, respectively, that of CaM-bound wild-type nNOS, and the E762R, E819R, and D813R mutants, whose activities were about 65% that of CaM-bound wild-type nNOS. The latter three mutants had normal K_m values for cytochrome *c* (data not shown), suggesting that their lower activities were not due to an impaired interaction with cytochrome *c*. Together, the data indicate that charge neutralization at Glu^{762}, Asp^{813}, and possibly Glu^{819} increases the activity of CaM-bound nNOS, whereas charge reversal at these same sites diminishes activity.

Fig. 4 also reports the cytochrome *c* reductase activities of the Arg^{1229} mutants. The CaM-free R1229N and R1229A mutants had only slightly higher activities compared with CaM-free wild-type nNOS, suggesting that Arg^{1229} is not so important for repressing activity in the CaM-free state. However, the activities of the CaM-bound R1229A and R1229N mutants were only 20% that of CaM-bound wild-type nNOS, indicating that Arg^{1229} enables nNOS to increase activity in response to CaM.

NADPH Oxidase Activity of the CaM-free Mutants—Almost all of the CaM-free mutants oxidized NADPH at rates that exceeded wild-type nNOS (Fig. 5), despite their not synthesizing detectable NO under this circumstance (data not shown). The NADPH oxidation rates of the CaM-free E762N, E762A, and E816R mutants were highest and were 12–18 times faster than the wild-type value. The NADPH oxidation rates of the CaM-free R1229N and R1229A mutants were also four to seven times faster than that of wild-type nNOS (Fig. 5). Because the NADPH oxidase activity of CaM-free nNOS is directly linked to the autoxidation rate of its reduced flavins (35, 36), our results establish that electronegative charged residues at the FNR/FMN module interface are required to minimize flavin autoxidation and the consequent generation of reduced oxygen species by nNOS.

NO Synthesis and NADPH Oxidation by the CaM-bound Mutants—Eleven of the 18 FMN surface mutants had a 30% or greater reduction in their NO synthesis activities relative to the wild-type activity (Fig. 6, *left panel*). The mutants with the lowest NO synthesis activities were, in decreasing order, E762R and

E816A (40% of the wild-type activity), E816R and E819A (32% of the wild-type activity), and E762A (21% of the wild-type activity). Substitution of three of the residues (Glu^{762}, Glu^{816}, and Glu^{819}) with Ala or Arg diminished NO synthesis activity, whereas substitution with Asn either had little effect or, in one case (E762N), doubled the NO synthesis activity relative to the wild-type activity. The NO synthesis activities of the complementary FNR surface mutants R1229N and R1229A were 23% and 34% that of wild-type nNOS, respectively. Thus, charged residues at the FNR/FMN module interface are important for maintaining NO synthesis activity in nNOS.

Fig. 6 (*right panel*) reports the NADPH oxidation rates during NO synthesis from L-Arg by the mutants and wild-type nNOS. Several mutants had higher rates of NADPH oxidation despite their lower rates of NO synthesis. Wild-type nNOS oxidized 2.0 molecules of NADPH/molecule of NO formed, which is close to the theoretical minimum of 1.5 (1, 4). The E819A, E819R, and E762A mutants had NADPH:NO stoichiometric ratios of greater than 3.5, indicating an NADPH consumption significantly beyond that required for NO synthesis. The NADPH oxidation rates of the R1229N and R1229A FNR surface mutants were also in excess of that required for NO synthesis. Thus, the electrostatic charge of these residues appears to be important for coupling NADPH consumption to NO synthesis.

Rates of Heme Reduction—To examine mutational effects on electron transfer, we measured the rate of heme reduction in single turnover reactions that were run in a stopped-flow spectrophotometer at 10 °C. Reactions were initiated by mixing CaM-bound enzymes with excess NADPH under a N_2/CO atmosphere. For comparison, we also ran reactions in which heme reduction was triggered by mixing Ca^{2+} and CaM with each NADPH-reduced enzyme. The rates of heme reduction were determined by following the absorbance increase at 444 nm *versus* time, which tracked formation of the ferrous heme-CO complex. As shown in Fig. 7, all of the mutants had slower heme reduction rates compared with wild-type nNOS, consistent with many of them having lower NO synthesis activities. In some cases, the heme reduction rate did not correspond well with the NO synthesis rate. This was most prominent for the Glu^{762} mutants, which had slower than expected rates of heme reduction and, to a lesser extent, for the Glu^{816} and Glu^{790} mutants. The heme reduction rates for the R1229A and R1229N FNR surface mutants were also slower than that of wild-type nNOS, consistent with their lower NO synthesis activities.

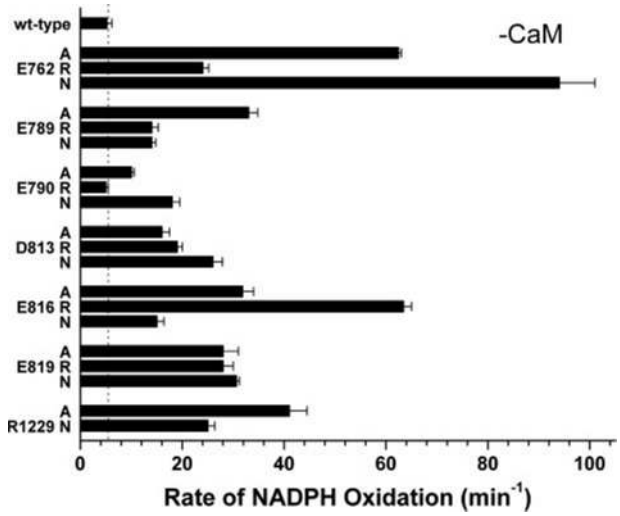

FIGURE 5. **Steady-state NADPH oxidase activities of nNOS and mutants in the absence of CaM.** Measurements were done at 25 °C. Assay conditions are described under "Experimental Procedures." Values represent the means ± S.D. of three independent measurements. The *dotted line* indicates the activity of wild-type (*wt-type*) nNOS.

DISCUSSION

Our results indicate that the electronegative surface patch of the FMN module plays a significant role in controlling electron transfer and catalysis in nNOS. Mutations that neutralized or reversed the electronegative charge of six surface residues on

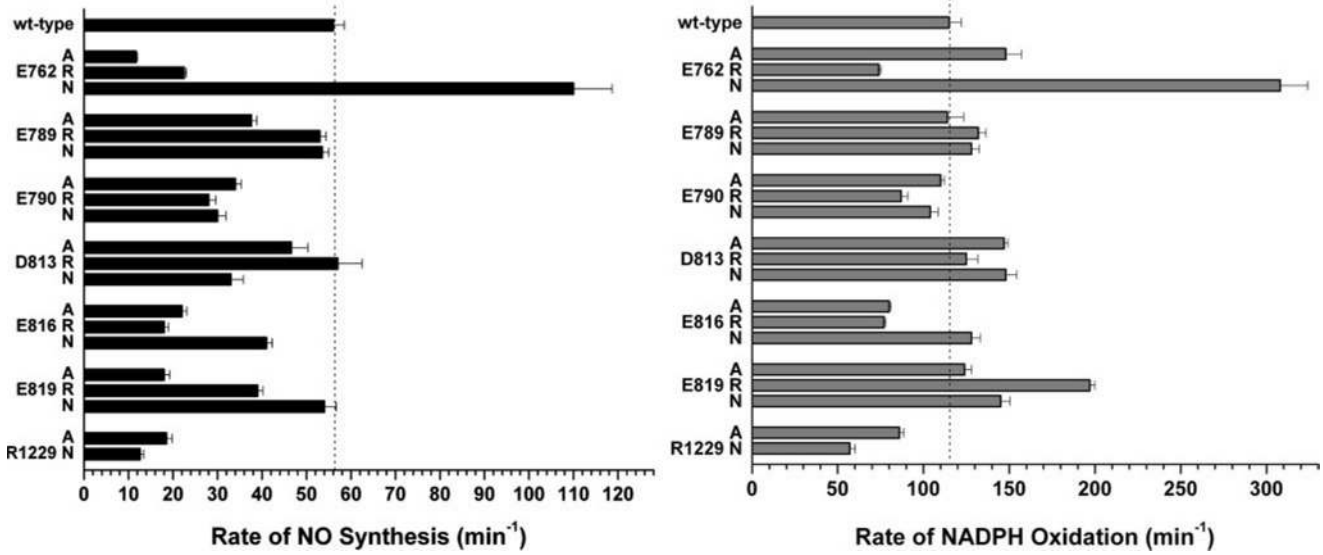

FIGURE 6. **Steady-state NO synthesis (*left panel*) and concurrent NADPH oxidation (*right panel*) activities of nNOS and mutants in the presence of CaM.** Measurements were done at 25 °C. Assay conditions are described under "Experimental Procedures." Values represent the means ± S.D. of three independent measurements. The *dotted lines* indicate the activity of wild-type (*wt-type*) nNOS.

the FMN module altered cytochrome *c* reduction, flavin autoxidation, heme reduction, and NO synthesis by nNOS. In general, the largest effects were seen in the Glu^{762} mutants, followed by the Glu^{816}, Glu^{819}, and Asp^{813} mutants and then the others (Glu^{790} and Glu^{789}), with the exact rank order often depending on whether CaM was bound or not and what aspect of catalysis was being considered.

Structure-Function Relationships—The six acidic residues are only partly conserved among NOS enzymes and related flavoproteins (Fig. 8). Remarkably, Glu^{762} is conserved among NOS enzymes but is replaced by neutral residues in related flavoproteins. Thus, Glu^{762} appears to be a key controlling residue that is specific to NOS enzymes. In contrast, the acidic residues Asp^{813} and Glu^{816} in nNOS are the best conserved among NOS enzymes and in related flavoproteins, whereas the acidic residues Glu^{789}, Glu^{790}, and Glu^{819} are partly conserved.

Despite the high impact of Glu^{762} on catalysis and electron transfer, this residue makes no observable salt bridge or hydrogen-bonding contacts with the FNR module in the nNOSr crystal structure (Fig. 3*C*). However, it is important to note that structural comparisons of the nNOSr, cytochrome P450 reductase, and cytochrome P450 reductase mutant x-ray structures (15) reveal significant rigid-body motions of their FMN modules relative to their FNR partners, thus highlighting the plasticity of these interfaces. Therefore, although a slight movement could enable a salt bridge interaction to occur between Glu^{762} and Arg^{1229} in nNOS, more work is required to judge the significance of this possibility. Indeed, Glu^{816}, which makes a clear salt bridge contact with Arg^{1229} in the nNOSr structure (15), had lesser mutation phenotypes than Glu^{762} in our study. As might be expected, the properties of the R1229A FNR surface mutant were comparable with those of the complementary interacting mutants (*i.e.* at Glu^{816}), particularly in the CaM-free state. In contrast, the properties of the CaM-free and CaM-bound Glu^{762} mutants diverged from those of the R1229A mutant, suggesting that other interactions of Glu^{762} are in play. Notably, the Glu^{816}–Arg^{1229} salt bridge is the only electrostatic interaction found in nNOS that is also conserved in cytochrome P450 reductase, which contains four additional unique salt bridges (10). Thus, our data reveal that the interactions of the NOS-specific residue Glu^{762} play a predominant role and may combine with a more generally conserved salt bridge interaction between Glu^{816} and Arg^{1229} to govern electron transfer and catalysis in nNOS. Curiously, in inducible NOS, the residue corresponding to Glu^{816} is a Ser (Fig. 8). Because this substitution eliminates the salt bridge contact with Arg^{1229}, it implies that the NOS-specific residue Glu^{762} may have an even more prominent role in governing inducible NOS catalysis.

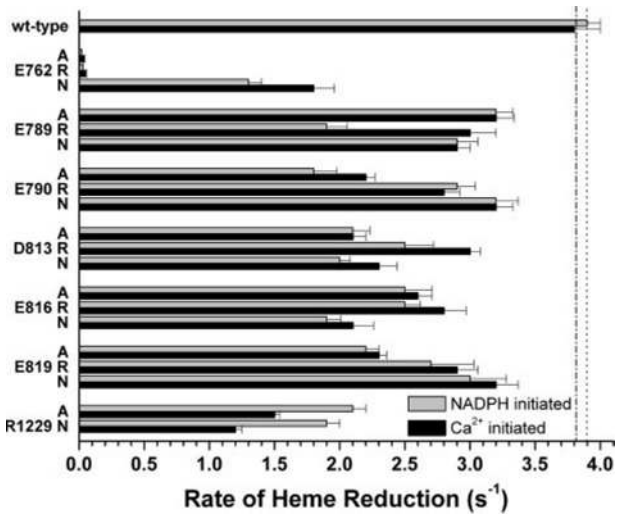

FIGURE 7. **Ferric heme reduction rates in nNOS and mutants.** Reactions were run at 10 °C in a stopped-flow spectrophotometer under anaerobic conditions and in the presence of CO. Heme reduction was triggered by either NADPH or $CaCl_2$ addition as described under "Experimental Procedures." Values are the means ± S.D. of experiments using two different batches of protein for each mutant, with eight separate reactions for each batch.

Effects on Interactions of the Six Acidic Surface Residues of the FMN Module—We consider that the six acidic surface residues are likely involved in two distinct subdomain interactions of the FMN module (FNR/FMN, FMN/oxygenase domain), and in the case of the cytochrome *c* reductase activity, there is also the interaction between the FMN module and cytochrome *c* itself. From our data, there is no way to directly know how the mutations impact the NOS subdomain or protein-protein interactions, which would require biophysical measures or further crystallography beyond the scope of the study. That said, our current data can indirectly report on some of these interactions. There is previously published evidence that the cytochrome *c* reductase activity of CaM-free nNOS is directly related to the degree of FMN shielding from solvent (16, 17), which in turn is

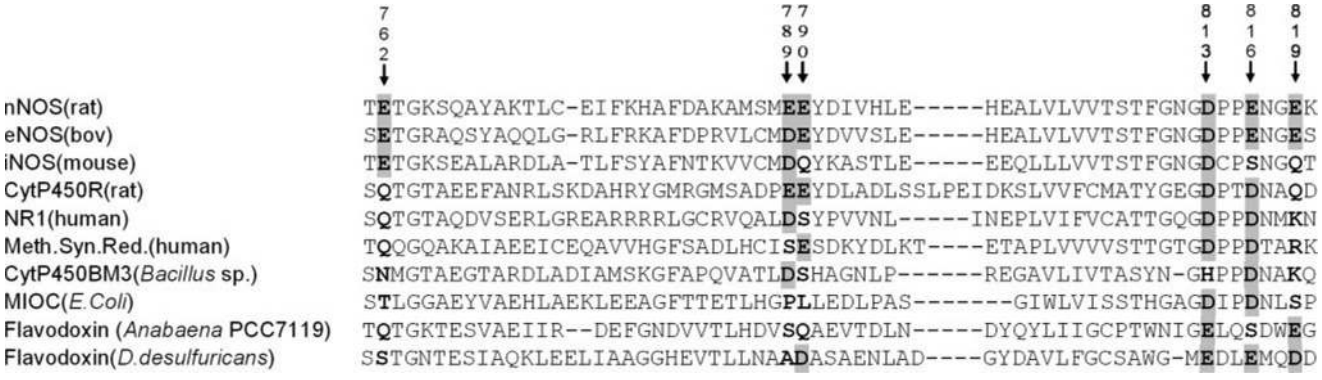

FIGURE 8. **Conservation of the six electronegative surface residues of the nNOS FMN module among related flavoproteins.** Numbered positions in *boldface* refer to the sequence of rat nNOS. Negatively charged residues are highlighted by *gray shading*. *eNOS*, bovine endothelial NOS; *iNOS*, murine inducible NOS; *CytP450R*, rat cytochrome P450 reductase; *NR1*, human novel reductase-1; *Meth.Syn.Red.*, human methionine synthase reductase; *CytP450BM3*, *Bacillus* cytochrome P450BM3; *MIOC*, *E. coli* flavodoxin MioC.

determined by the stability of the FNR/FMN subdomain interaction depicted in the nNOSr crystal structure. Thus, the reductase activities we measured under CaM-free conditions can provide a hierarchy for how mutations that neutralize the charge of each residue impact the stability of the FNR/FMN subdomain interaction. As indicated in Fig. 4 (*left panel*), neutralizing mutations at Glu^{762} clearly had the greatest impact, whereas neutralization of each of the other residues had a lesser or similar impact.

Within this context, we likely can discount any possible thermodynamic effects that the mutations might have on FMN reduction potentials because the reduction potential of cytochrome *c* is so positive that there will always be a sufficient driving force for its reduction. Besides, the mutants all had increased reductase activity relative to the wild-type activity, which cannot be reconciled on the basis of a change in FMN reduction potentials. We can also discount any effects of the mutations on FMN module interaction with cytochrome *c* itself. The binding affinity of nNOS for cytochrome *c* is such that, under the conditions of assay (excess of cytochrome *c*), the reductase activity is independent of increases in cytochrome *c* concentration, and again, we observed the activities of the mutants to increase instead of decrease.

Altered Reductase and Oxidase Activities and Flavin Autoxidation in the Mutants—Remarkably, 20 of the 21 mutants had increased cytochrome *c* reductase and NADPH oxidase activities in the CaM-free state. The mutational effects on these two distinct catalytic activities had a very similar rank order in the CaM-free enzymes (compare Figs. 4 (*left panel*) and 5), implying a common mechanism of influence. Given that the cytochrome *c* reductase activity of CaM-free nNOS is determined by a conformational equilibrium between shielded and deshielded states of the FMN module (16, 18), one possibility is that the mutations have shifted the conformational equilibrium toward the FMN-deshielded state. According to this model, neutralizing or reversing the electronegative surface charges of the FMN module may significantly weaken its interaction with the FNR module, thus deshielding the FMN module and enabling faster electron flux to cytochrome *c* in the CaM-free state. The observed trend toward lesser salt effects on individual mutant reductase activities is also consistent with a model in which the charge interactions of these residues help to govern the conformational equilibrium of the FMN module. Further work is under way to substantiate this model.

Regarding the higher NADPH oxidase activities of the CaM-free mutants, under this condition, the NADPH oxidase activity is determined by the rate at which the reduced flavins react with O_2. Normally, the rate of flavin autoxidation is quite slow ($\sim$3–5 min^{-1} at 25 °C) (35, 36), which demonstrates that NOS enzymes have evolved efficient mechanisms to protect their reduced flavins from autoxidation. Apparently, the electronegative surface patch of the FMN module is part of a mechanism that protects the reduced flavins from O_2, with particularly essential contributions provided by Glu^{816} and Glu^{762} in CaM-free nNOS. Whether the protective mechanism involves a precise tuning of FMN module shielding is a possibility that can now be addressed. In the CaM-bound mutants, neutralizing the negative charge of Glu^{762}, Glu^{819}, or Asp^{813} (by Ala or Asn substitution) increased the cytochrome *c* reductase activity beyond the wild-type value, whereas reversing the charge of any of these three residues (by Arg substitution) diminished the activity compared with the wild-type activity.

In some cases, the mutational effect on cytochrome *c* reductase activity in the CaM-bound enzymes differed from the effect observed for the same mutation in the CaM-free enzymes. This is particularly true for the R1229A mutant and for the charge-reversing mutations at Glu^{762}, Glu^{819}, and Asp^{813}, which all increased activity relative to the wild-type activity under CaM-free conditions and decreased activity relative to the wild-type activity under CaM-bound conditions. Such divergent mutational effects could occur if the reductase activity is subject to a different rate-limiting step in the CaM-free *versus* CaM-bound condition, as has been proposed previously (16, 18), and if these mutations have opposite effects on either rate-limiting step. This possibility can now be investigated. In any case, the results show that electron flux through the FMN module is sensitive to changes in the electrostatics at the FNR/FMN interface, such that relatively small changes introduced by point mutation can either increase or decrease electron flux through the CaM-bound enzyme.

Heme Reduction and NO Synthesis in the Mutants—NOS heme reduction relies on a productive interaction between the FMN and NOS oxygenase subdomains. A previous mutagenesis study suggests that this involves electrostatic interaction between surface residues of the FMN module and electropositive residues of the NOS oxygenase domain (37).

Measuring heme reduction rates is an indirect way to identify which of the six acidic surface residues may aid the interaction of the FMN module with the NOS oxygenase domain for heme reduction and NO synthesis (31). Although comparing rates of heme reduction is superior to NO synthesis activities in this regard (38), heme reduction could still be subject to possible mutant effects on FMN reduction potentials given there is a relatively weak driving force for heme reduction by $FMNH_2$ in nNOS (39).

Because none of mutations enabled NO synthesis in the absence of CaM, we can conclude that the electronegative surface patch of the FMN module is not required to prevent heme reduction in CaM-free nNOS. This is consistent with the autoinhibitory insert and C-terminal regulatory elements being required to block heme reduction in CaM-free NOS (26, 35, 40). Regarding heme reduction in the CaM-bound mutants, Glu^{762} is clearly the most important of the six acidic residues because Arg and Ala substitutions at this position slowed down nNOS heme reduction by 95% and caused corresponding decreases in NO synthesis activity. In comparison, mutations of the other five electronegative surface residues also decreased the heme reduction rate by 15–50% and thus had relatively weaker effects. Our findings suggest that the individual interactions of these five residues may not be as important as the interactions of the NOS-specific Glu^{762} residue for enabling heme reduction by the FMN module. Further work to substantiate this possibility and to determine any thermodynamic effects of the mutations is under way.

Slower heme reduction rates in the CaM-bound mutants correlated with lower NO synthesis activities in most cases,

consistent with ferric heme reduction being the rate-limiting step (3, 38). The one clear exception was the E762N mutant, which had a 50% slower heme reduction rate despite its having an NO synthesis activity that was twice that of the wild-type nNOS activity. The mechanism that enables this unusual combination is under investigation and will be reported elsewhere.

Several CaM-bound mutants had NADPH oxidation rates that were significantly higher than what is required for their NO synthesis (1.5 molecules of NADPH/molecule of NO formed), indicating they have an uncoupled NADPH oxidation. These were, in rank order, E762A (12.6 NADPH/NO), E819A (6.9), E819R (5.1), D813N (4.5), and E816R (4.3). These same mutants also had greater NADPH consumption in the absence of CaM (Fig. 5), although the rank order was somewhat different in that case. Thus, we suspect that the reduced flavins in these CaM-bound mutants are still undergoing relatively fast autoxidation while trying to provide electrons to the NOS heme for NO synthesis. One can estimate if their increased flavin autoxidation rates measured in the absence of CaM can account for the extra NADPH consumed during NO synthesis by subtracting the NADPH oxidation rate observed in the CaM-free state from the rate observed in the CaM-bound state during NO synthesis. For most mutants, this calculation lowers their NADPH/NO stoichiometry such that 1.8–3.5 molecules of NADPH were consumed per molecule of NO formed, which is normal or approaching normal. However, three of the CaM-bound mutants still show significant uncoupling even after subtracting their NADPH consumption under CaM-free conditions. These are the E762A (7.3 NADPH/NO), E819R (4.3), and E819A (5.3) mutants. This implies that CaM binding may further increase their flavin autoxidation rates or that additional uncoupling mechanisms that involve the heme are in play. This latter possibility is unlikely because the mutations are in the NOS reductase domain and should not affect heme function. We suspect that flavin autoxidation is so fast in these three CaM-bound mutants that O_2 can effectively compete with the NOS oxygenase heme for electrons from the FMN hydroquinone. This would diminish electron flux to the heme and lower the NO synthesis activity relative to the NADPH consumed. These possibilities can now be addressed. In any case, our data establish that the electronegative patch residues of the FMN module have a central role in minimizing flavin autoxidation in both the resting (CaM-free) and catalytically active (CaM-bound) nNOS.

Relationship to Other Flavoproteins—Why do some NOS enzymes maintain extensive electrostatic charge complementarity between their FMN and FNR modules? After all, bacterial cytochrome P450BM3 has attached heme and flavoprotein domains as in NOS but has markedly less electronegative charge on its FMN module interface. Presumably, having covalently attached electron transfer domains should eliminate the pressure to maintain strong interdomain contacts. Indeed, the fact that the heme reduction rate in P450BM3 (13) is ~24 times faster than in nNOS argues that interdomain electrostatic complementation is not essential for good rates of electron transfer in a flavoheme enzyme like NOS. The opposite situation holds for the flavodoxins, which maintain a more extensive electronegative surface patch that appears to aid their interactions with physically separate electron donor and acceptor proteins during catalysis (21). Related dual-flavin reductases like cytochrome P450 reductase and sulfite reductase also maintain electrostatic complementation at their FMN module interfaces (10, 24), possibly to aid interaction with their unattached electron acceptor proteins. On the basis of comparison with P450BM3, we wondered if the electrostatic complementation between the FMN and FNR modules in nNOS is maintained to impede its rate of heme reduction, which has to remain relatively slow for the enzyme to release the NO that it makes (38). However, our current data show that this is not the case. Rather, the electronegative patch residues are required to minimize autoxidation of reduced flavins in nNOS. This is particularly important for NOS enzymes because their heme reduction is so slow that reduced flavins build up in the enzyme during catalysis. Moreover, enzyme-generated NO can directly react with reduced oxygen species like superoxide to produce the cellular toxin peroxynitrite (41). It is worth noting that, in P450BM3, there is very little NADPH oxidation in the absence of the substrate (13) despite reduced flavins building up under this circumstance. This implies that flavin autoxidation in dual-flavin enzymes can be minimized by a variety of mechanisms. Perhaps hydrophobic surface contacts help to maintain the subdomain interaction. P450BM3 also relies on the FMN semiquinone to transfer electrons to its heme while kinetically blocking the electron transfer reactions of $FMNH_2$ (14, 22). Whether this strategy helps to minimize flavin autoxidation during catalysis is an alternative possibility.

REFERENCES

1. Griffith, O. W., and Stuehr, D. J. (1995) *Annu. Rev. Physiol.* **57,** 707–736
2. MacMicking, J., Xie, Q. W., and Nathan, C. (1997) *Annu. Rev. Immunol.* **15,** 323–350
3. Masters, B. S., McMillan, K., Sheta, E. A., Nishimura, J. S., Roman, L. J., and Martásek, P. (1996) *FASEB J.* **10,** 552–558
4. Andrew, P. J., and Mayer, B. (1999) *Cardiovasc. Res.* **43,** 521–531
5. Wei, C.-C., Crane, B. R., and Stuehr, D. J. (2003) *Chem. Rev.* **103,** 2365–2383
6. Abu-Soud, H. M., and Stuehr, D. J. (1993) *Proc. Natl. Acad. Sci. U. S. A.* **90,** 10769–10772
7. Gachhui, R., Presta, A., Bentley, D. F., Abu-Soud, H. M., McArthur, R., Brudvig, G., Ghosh, D. K., and Stuehr, D. J. (1996) *J. Biol. Chem.* **271,** 20594–20602
8. Klatt, P., Heinzel, B., John, M., Kastner, M., Bohme, E., and Mayer, B. (1992) *J. Biol. Chem.* **267,** 11374–11378
9. Newman, E., Spratt, D. E., Mosher, J., Cheyne, B., Montgomery, H. J., Wilson, D. L., Weinberg, J. B., Smith, S. M., Salerno, J. C., Ghosh, D. K., and Guillemette, J. G. (2004) *J. Biol. Chem.* **279,** 33547–33557
10. Wang, M., Roberts, D. L., Paschke, R., Shea, T. M., Siler Masters, B. S., and Kim, J.-J. P. (1997) *Proc. Natl. Acad. Sci. U. S. A.* **94,** 8411–8416
11. Finn, R. D., Basran, J., Roitel, O., Wolf, C. R., Munro, A. W., Paine, M. J., and Scrutton, N. S. (2003) *Eur. J. Biochem.* **270,** 1164–1175
12. Olteanu, H., Wolthers, K. R., Munro, A. W., Scrutton, N. S., and Banerjee, R. (2004) *Biochemistry* **43,** 1988–1997
13. Munro, A. W., Daff, S., Coggins, J. R., Lindsay, J. G., and Chapman, S. K. (1996) *Eur. J. Biochem.* **239,** 403–409
14. Sevrioukova, I., Shaffer, C., Ballou, D. P., and Peterson, J. A. (1996) *Biochemistry* **35,** 7058–7068
15. Garcin, E. D., Bruns, C. M., Lloyd, S. J., Hosfield, D. J., Tiso, M., Gachhui, R., Stuehr, D. J., Tainer, J. A., and Getzoff, E. D. (2004) *J. Biol. Chem.* **279,** 37918–37927
16. Konas, D. W., Zhu, K., Sharma, M., Aulak, K. S., Brudvig, G. W., and Stuehr, D. J. (2004) *J. Biol. Chem.* **279,** 35412–35425

17. Grunau, A., Paine, M. J., Ladbury, J. E., and Gutierrez, A. (2006) *Biochemistry* **45,** 1421–1434
18. Craig, D. H., Chapman, S. K., and Daff, S. (2002) *J. Biol. Chem.* **277,** 33987–33994
19. Tiso, M., Konas, D. W., Panda, K., Garcin, E. D., Sharma, M., Getzoff, E. D., and Stuehr, D. J. (2005) *J. Biol. Chem.* **280,** 39208–39219
20. Govindaraj, S., and Poulos, T. L. (1995) *Biochemistry* **34,** 11221–11226
21. Hall, D. A., Vander Kooi, C. W., Stasik, C. N., Stevens, S. Y., Zuiderweg, E. R., and Matthews, R. G. (2001) *Proc. Natl. Acad. Sci. U. S. A.* **98,** 9521–9526
22. Hanley, S. C., Ost, T. W., and Daff, S. (2004) *Biochem. Biophys. Res. Commun.* **325,** 1418–1423
23. Shen, A. L., and Kasper, C. B. (1995) *J. Biol. Chem.* **270,** 27475–27480
24. Sibille, N., Blackledge, M., Brutscher, B., Coves, J., and Bersch, B. (2005) *Biochemistry* **44,** 9086–9095
25. Zhang, J., Martásek, P., Paschke, R., Shea, T., Siler Masters, B. S., and Kim, J.-J. P. (2001) *J. Biol. Chem.* **276,** 37506–37513
26. Nishida, C. R., and Ortiz de Montellano, P. R. (2001) *J. Biol. Chem.* **276,** 20116–20124
27. Schrammel, A., Gorren, A. C., Stuehr, D. J., Schmidt, K., and Mayer, B. (1998) *Biochim. Biophys. Acta* **1387,** 257–263
28. Crane, B. R., Arvai, A. S., Ghosh, D. K., Wu, C., Getzoff, E. D., Stuehr, D. J., and Tainer, J. A. (1998) *Science* **279,** 2121–2126
29. Adak, S., Ghosh, S., Abu-Soud, H. M., and Stuehr, D. J. (1999) *J. Biol. Chem.* **274,** 22313–22320
30. Adak, S., Santolini, J., Tikunova, S., Wang, Q., Johnson, J. D., and Stuehr, D. J. (2001) *J. Biol. Chem.* **276,** 1244–1252
31. Panda, K., Adak, S., Konas, D., Sharma, M., and Stuehr, D. J. (2004) *J. Biol. Chem.* **279,** 18323–18333
32. Ghosh, D. K., Wu, C., Pitters, E., Moloney, M., Werner, E. R., Mayer, B., and Stuehr, D. J. (1997) *Biochemistry* **36,** 10609–10619
33. Adak, S., Aulak, K. S., and Stuehr, D. J. (2001) *J. Biol. Chem.* **276,** 23246–23252
34. Stuehr, D. J., and Ghosh, S. (2000) in *Nitric Oxide* (Mayer, B., ed) pp. 33–70, Springer-Verlag, Berlin
35. Roman, L. J., Martásek, P., Miller, R. T., Harris, D. E., de la Garza, M. A., Shea, T. M., Kim, J.-J. P., and Siler Masters, B. S. (2000) *J. Biol. Chem.* **275,** 29225–29232
36. Stuehr, D., Pou, S., and Rosen, G. M. (2001) *J. Biol. Chem.* **276,** 14533–14536
37. Shimanuki, T., Sato, H., Daff, S., Sagami, I., and Shimizu, T. (1999) *J. Biol. Chem.* **274,** 26956–26961
38. Stuehr, D. J., Santolini, J., Wang, Z.-Q., Wei, C.-C., and Adak, S. (2004) *J. Biol. Chem.* **279,** 36167–36170
39. Daff, S. (2003) *Biochem. Soc. Trans.* **31,** 502–505
40. Chen, P.-F., and Wu, K. K. (2003) *J. Biol. Chem.* **278,** 52392–52400
41. Porasuphatana, S., Tsai, P., and Rosen, G. M. (2003) *Comp. Biochem. Physiol. C Toxicol. Pharmacol.* **134,** 281–289